

SIC-Based Hybrid Pre-Coding For MM-Wave MIMO Systems

¹ Abdul Wase Mohammed, ² Mohammed Abdul Muqet, ³ Mohd Sayeeduddin Habeeb.

Lecturer's Department of Electrical Engineering, King Khalid University, Abha, Kingdom of Saudi Arabia.

Abstract: Millimeter wave (MM Wave) MIMO can possible use hybrid analog and digital precoding, that uses atiny low variety of RF chains to cut back the energy consumption related to mixed signal parts like analog-to-digital parts to not mention baseband process quality. However, most hybrid precoding techniques think about a totally connected design requiring an outsized variety of part shifters, That is additionally energy-intensive. During this paper, we tend to concentrate on the additional energy economical hybrid precoding with subconnected design, and propose a sequential interference cancelation (SIC)-based hybrid precoding with near-optimal performance and low quality. Impressed by the concept of set on for multiuser detection, we tend to 1st propose to decompose the whole possible rate optimization downside with nonconvex constraints into a series of easy subrateoptimisation issues; every of that solely considers one subantenna array. Then, we tend to prove that increasing the possible substrate of every subantenna array is similar to merely seeking a precoding vector sufficiently shut (in terms of geometrician distance) to the free best answer. Finally, we tend to propose a low-complexity formula to appreciate SIC-based hybrid precoding, which may avoid the requirement for the singular price decomposition (SVD) and matrix operation. Quality analysis shows that the quality of SIC-based hybrid precoding is simply concerning 100 percent as advanced as that of the recently planned spatially distributed precoding in typical mmWave MIMO systems. Simulation results verify that SIC-based hybrid precoding is near-optimal and enjoys higher energy potency than the spatially distributed precoding and also the absolutely digital precoding.

Index Terms: MIMO, mmWave communications, hybrid precoding, energy-efficient, 5G.

I. INTRODUCTION

THE integration of millimeter-wave (mmWave) and massive multiple-input multiple-output (MIMO) technique can achieve orders of magnitude increase in system throughput due to larger bandwidth [1] and higher spectral efficiency [2], which makes it promising for future 5G wireless communication systems [3]. On one hand, massive MIMO with a very large antenna array (e.g., 256 antennas) at the base station (BS) can simultaneously serve a set of users through the use of precoding [4]. It has been theoretically proved that massive MIMO can achieve orders of magnitude increase in spectral efficiency, since it can provide more multi-user gain [2]. On the other hand, mmWave with high frequencies enables such large antenna array in massive MIMO to be packed in small physical dimension [5]. Furthermore, the large antenna array can also provide sufficient array gain by precoding [6], [7] to overcome the free-space pathloss of mmWave signals and establish links with satisfying signal-to-noise ratio (SNR) [8]. For MIMO in conventional cellular frequency band (e.g., 2–3 GHz), precoding is entirely realized in the digital domain to cancel interference between different data streams. For a conventional digital precoding, each antenna requires a dedicated energy-intensive radio frequency (RF) chain (including digital-to-analog converter, up converter, etc.), whose energy consumption is a large

part (about 250 mW per RF chain [9]) of the total energy consumption at mmWave frequencies due to the wide bandwidth. If the conventional digital precoding is applied in mmWave massive MIMO system with a large number of antennas, the corresponding large number of RF chains will bring high energy consumption, e.g., 16 W is required by a mmWave massive MIMO system with 64 antennas.

To solve this problem, the hybrid analog and digital precoding has been proposed [10]. The key idea is to divide the conventional digital precoder into a small-size digital precoder (realized by a small number of RF chains) to cancel interference and a large-size analog precoder (realized by a large number of analog phase shifters (PSs)) to increase the antenna array gain. In this way, hybrid precoding can reduce the number of required RF chains without obvious performance loss, which makes it enjoy much higher energy efficiency than digital precoding [10]. The existing hybrid precoding schemes can be divided into two categories. The first category of hybrid precoding based on spatially sparse precoding was proposed in [11]–[13], which formulated the achievable rate optimization problem as a sparse approximation problem and solved it by the orthogonal matching pursuit (OMP) algorithm [14] to achieve the near-optimal performance. The second category of hybrid

precoding based on codebooks was proposed in [15]–[17], which involved an iterative searching procedure among the predefined codebooks to find the optimal hybrid precoding matrix.

However, these algorithms are all designed for the hybrid precoding with the fully-connected architecture, where each RF chain is connected to all BS antennas via PSs. As the number of BS antennas is very large (e.g., 256 as considered in [11]), the fully-connected architecture requires thousands of PSs, which may bring three additional limitations: 1) it consumes more energy for excitation like the giant phased array radar [18]; 2) it requires more energy to compensate for the insertion loss of PS [18]; 3) it involves higher computational complexity, which will also bring more energy consumption [19]. In contrast, the hybrid precoding with the sub-connected architecture, where each RF chain is connected to only a subset of BS antennas, can significantly reduce the number of required PSs. Therefore, the sub-connected architecture is expected to be more energy efficient and easier to be implemented for mmWave MIMO systems. Unfortunately, designing the optimal hybrid precoding with the sub-connected architecture is still a challenging problem [10], [20], since such architecture changes the constraints on the original problem of hybrid precoding with the fully-connected architecture.

In this paper, we propose a successive interference cancellation (SIC)-based hybrid precoding with sub-connected architecture. The contributions of this paper can be summarized as follows.

- Inspired by the idea of SIC derived for multi-user signal detection [21], we propose to decompose the total achievable rate optimization problem with non-convex constraints into a series of simple sub-rate optimization problems, each of which only considers one sub-antenna array. Then, we maximize the achievable sub-rate of each sub-antenna array one by one until the last sub-antenna array is considered.
- We prove that maximizing the achievable sub-rate of each sub-antenna array is equivalent to seeking a precoding vector which has the smallest Euclidean distance to the unconstrained optimal solution. Based on this fact, we can easily obtain the optimal precoding vector for each sub-antenna array.
- We further propose a low-complexity algorithm to realize the SIC-based precoding, which avoids the need for singular value decomposition (SVD) and matrix inversion. Complexity evaluation shows that the complexity of SIC-based precoding is only about 10% as complex as that of the spatially

sparse precoding [11] in typical mmWave MIMO systems. Simulation results verify that the proposed SIC-based hybrid precoding is near-optimal and enjoys higher energy efficiency than the spatially sparse precoding [11] and the fully digital precoding.

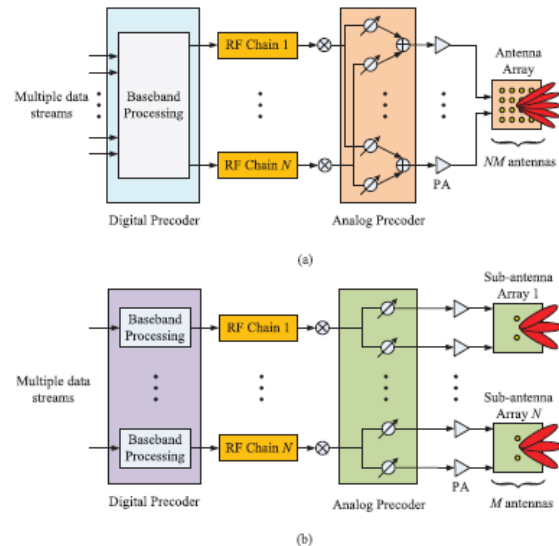


Fig. 1. Two typical architectures of the hybrid precoding in mmWave MIMO systems: (a) Fully-connected architecture, where each RF chain is connected to all BS antennas; (b) Sub-connected architecture, where each RF chain is connected to only a subset of BS antennas.

II. SYSTEM MODEL

Fig1 illustrates two typical architectures for hybrid precoding in mmWave MIMO systems, i.e., the fully-connected architecture as shown in Fig1 (a) and the sub-connected architecture as shown in Fig. 1 (b). In both cases the BS has N antennas but only N RF chains. From Fig1, we observe that the sub-connected architecture will likely be more energy-efficient, since it only requires N PSs, while the fully-connected architecture requires N^2 PSs. To fully achieve the spatial multiplexing gain, the BS usually transmits N independent data streams to users employing K receive antennas [10]. In the sub-connected architecture as shown in Fig. 1 (b), N data streams in the baseband are precoded by the digital precoder \mathbf{D} . In cases where complexity is a concern, \mathbf{D} can be further specialized to be a diagonal matrix as $\mathbf{D} = \text{diag}[d_1, d_2, \dots, d_N]$, where $d_n \in \mathbb{R}$ for $n = 1, 2, \dots, N$ [10]. Then the role of \mathbf{D} essentially performs some power allocation. After passing through the corresponding RF chain, the digital-domain signal from each RF chain is delivered to only M PSs [22] to perform the analog precoding, which can be denoted by

the analog weighting vector $\bar{\mathbf{a}}_n \in \mathbb{C}^{M \times 1}$, whose elements have the same amplitude $1/\sqrt{M}$ but different phases [22].

After the analog precoding, each data stream is finally transmitted by a sub-antenna array with only M antennas associated with the corresponding RF chain. Then, the received signal vector $\mathbf{y} = [y_1, y_2, \dots, y_K]^T$ at the user in a narrowband system can be presented as

$$\mathbf{y} = \sqrt{\rho} \mathbf{H} \mathbf{A} \mathbf{D} \mathbf{s} + \mathbf{n} = \sqrt{\rho} \mathbf{H} \mathbf{P} \mathbf{s} + \mathbf{n}, \quad (1)$$

where ρ is the average received power; $\mathbf{H} \in \mathbb{C}^{K \times NM}$ denotes the channel matrix, \mathbf{A} is the $NM \times N$ analog precoding matrix comprising N analog weighting vectors $\{\bar{\mathbf{a}}_m\}_{m=1}^N$ as

$$\mathbf{A} = \begin{bmatrix} \bar{\mathbf{a}}_1 & \mathbf{0} & \dots & \mathbf{0} \\ \mathbf{0} & \bar{\mathbf{a}}_2 & & \mathbf{0} \\ \vdots & & \ddots & \vdots \\ \mathbf{0} & \mathbf{0} & \dots & \bar{\mathbf{a}}_N \end{bmatrix}_{NM \times N}, \quad (2)$$

$\mathbf{s} = [s_1, s_2, \dots, s_N]^T$ represents the transmitted signal vector in the baseband. In this paper, we assume the widely used Gaussian signals [10]–[13], [15]–[17] with normalized signal power $\mathbb{E}(\mathbf{s}\mathbf{s}^H) = \frac{1}{N} \mathbf{I}_N$, while the practical system with finite alphabet inputs [23], [24] will be also briefly discussed in Section IV. $\mathbf{P} = \mathbf{A}\mathbf{D}$ presents the hybrid precoding matrix of size $NM \times N$, which satisfies $\|\mathbf{P}\|_F \leq N$ to meet the total transmit power constraint [11]. Finally, $\mathbf{n} = [n_1, n_2, \dots, n_N]^T$ is an additive white Gaussian noise (AWGN) vector, whose entries follow the independent and identical distribution (i.i.d.) $\mathcal{CN}(0, \sigma^2)$. It is known that mmWave channel \mathbf{H} will not likely follow the rich-scattering model assumed at low frequencies due to the limited number of scatters in the mmWave propagation environment [3]. In this paper, we adopt the geometric Saleh-Valenzuela channel model to embody the low rank and spatial correlation characteristics of mmWave communications [10]–[13], [15]–[17], [25] as

$$\mathbf{H} = \gamma \sum_{l=1}^L \alpha_l \mathbf{\Lambda}_r(\phi_l^r, \theta_l^r) \mathbf{\Lambda}_t(\phi_l^t, \theta_l^t) \mathbf{f}_r(\phi_l^r, \theta_l^r) \mathbf{f}_t^H(\phi_l^t, \theta_l^t) \quad (3)$$

where $\gamma = \sqrt{\frac{NMK}{L}}$ is a normalization factor, L is the number of effective channel paths corresponding to the limited number of scatters, and we usually have $L \leq N$ for mmWave communication systems. $\alpha_l \in \mathbb{C}$ is the gain of the l th path. (θ_l^r) are the azimuth (elevation) angles of departure and arrival (AoDs/AoAs),

respectively. The transmit and receive antenna array gain at a specific AoD and AoA, respectively.

III. SIC-BASED HYBRID PRECODING FOR MMWAVE MIMO SYSTEMS

In this section, we propose a low-complexity SIC-based hybrid precoding to achieve the near-optimal performance. The evaluation of computational complexity is also provided to show its advantages over current solutions. A. Structure of SIC-based hybrid precoding In this paper, we aim to maximize the total achievable rate of mmWave MIMO systems [2], while other criteria such as the max-min fairness criterion [27] are also of interest. Specifically, R can be expressed as [11]

$$R = \log_2 \left(\mathbf{I}_K + \frac{\rho}{N\sigma^2} \mathbf{H} \mathbf{P} \mathbf{P}^H \mathbf{H}^H \right). \quad \dots\dots\dots (6)$$

According to the system model (1) in Section II, since the hybrid precoding matrix \mathbf{P} can be represented as $\mathbf{P} = \mathbf{A}\mathbf{D} = \text{diag}\{\bar{\mathbf{a}}_1, \dots, \bar{\mathbf{a}}_N\} \cdot \text{diag}\{d_1, \dots, d_N\}$, there are three constraints for the design of \mathbf{P} : Constraint 1: \mathbf{P} should be a block diagonal matrix similar to the form of \mathbf{A} as shown in (2), i.e., $\mathbf{P} = \text{diag}\{\bar{\mathbf{p}}_1, \dots, \bar{\mathbf{p}}_N\}$, where $\bar{\mathbf{p}}_n = d_n \bar{\mathbf{a}}_n$ is the $M \times 1$ non-zero vector of the n th column \mathbf{p}_n of \mathbf{P} , i.e., $\mathbf{p}_n = [\mathbf{0}_{1 \times M(n-1)}, \bar{\mathbf{p}}_n, \mathbf{0}_{1 \times M(N-n)}]^T$

Constraint 2: The non-zero elements of each column of \mathbf{P} should have the same amplitude, since the digital precoding matrix \mathbf{D} is a diagonal matrix, and the amplitude of non-zero elements of the analog precoding matrix \mathbf{A} is fixed to $1/\sqrt{M}$;

Constraint 3: The Frobenius norm of \mathbf{P} should satisfy $\|\mathbf{P}\|_F \leq N$ to meet the total transmit power constraint, where N is the number of RF chains equal to the number of transmitted data streams. Unfortunately, these non-convex constraints on \mathbf{P} make maximizing the total achievable rate (6) very difficult to be solved. The maximization sum-rate criterion can also suppress the interference as much as possible, and the mathematical quantification of such interference will be an important topic for future work. However, based on the special block diagonal structure of the hybrid precoding matrix \mathbf{P} , we observe that the precoding on different sub-antenna arrays are independent. This inspires us to decompose the total achievable rate (6) into a series of sub-rate optimization problems, each of which only considers one sub-antenna array.

In particular, we can divide the hybrid precoding matrix \mathbf{P} as $\mathbf{P} = [\mathbf{P}_{N-1} \mathbf{p}_N]$, where \mathbf{p}_N is the N th column of \mathbf{P} , and \mathbf{P}_{N-1} is an $NM \times (N-1)$ matrix containing the first $(N-1)$ columns of \mathbf{P} . Then, the total achievable rate R in (6) can be rewritten as

$$\begin{aligned} R &= \log_2 \left(\mathbf{I}_K + \frac{\rho}{N\sigma^2} \mathbf{H} \mathbf{P} \mathbf{P}^H \mathbf{H}^H \right) \\ &= \log_2 \left(\mathbf{I}_K + \frac{\rho}{N\sigma^2} \mathbf{H} [\mathbf{P}_{N-1} \mathbf{p}_N] [\mathbf{P}_{N-1} \mathbf{p}_N]^H \mathbf{H}^H \right) \\ &= \log_2 \left(\mathbf{I}_K + \frac{\rho}{N\sigma^2} \mathbf{H} \mathbf{P}_{N-1} \mathbf{P}_{N-1}^H \mathbf{H}^H \right. \\ &\quad \left. + \frac{\rho}{N\sigma^2} \mathbf{H} \mathbf{p}_N \mathbf{p}_N^H \mathbf{H}^H \right) \\ &\stackrel{(a)}{=} \log_2 (|\mathbf{T}_{N-1}|) + \log_2 \left(\mathbf{I}_K + \frac{\rho}{N\sigma^2} \mathbf{T}_{N-1}^{-1} \mathbf{H} \mathbf{p}_N \mathbf{p}_N^H \mathbf{H}^H \right) \\ &\stackrel{(b)}{=} \log_2 (|\mathbf{T}_{N-1}|) + \log_2 \left(1 + \frac{\rho}{N\sigma^2} \mathbf{p}_N^H \mathbf{H}^H \mathbf{T}_{N-1}^{-1} \mathbf{H} \mathbf{p}_N \right), \quad (7) \end{aligned}$$

where (a) is obtained by defining the auxiliary matrix

IV. RESULT

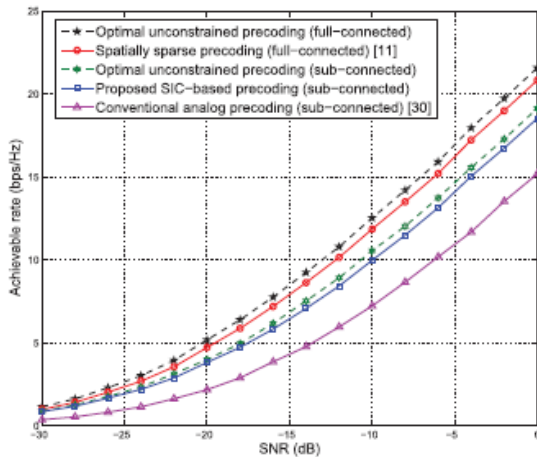


Fig. 3. Achievable rate comparison for an $NM \times K = 64 \times 16$ ($N = 8$) mmWave MIMO system.

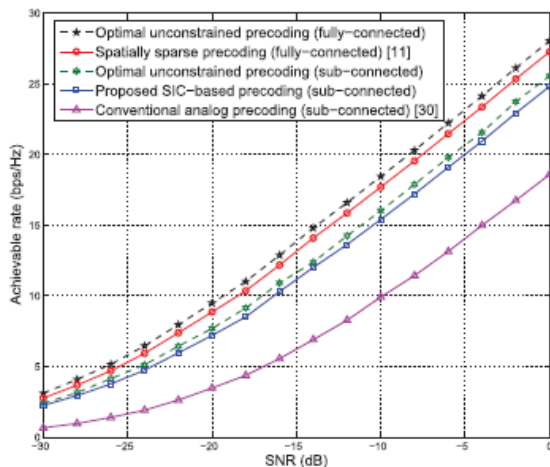


Fig. 4. Achievable rate comparison for an $NM \times K = 128 \times 32$ ($N = 16$) mmWave MIMO system.

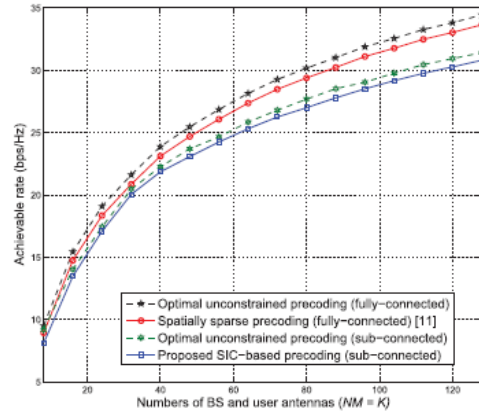


Fig. 5. Achievable rate comparison against the numbers of BS and user antennas ($NM = K$), where $N = 8$ and SNR = 0 dB.

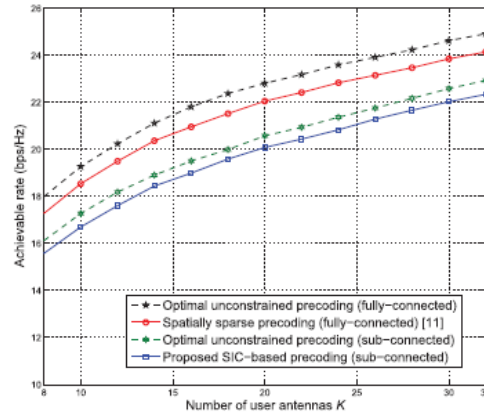


Fig. 6. Achievable rate comparison against the number of user antennas K , where $NM = 64$, $N = 8$, and SNR = 0 dB.

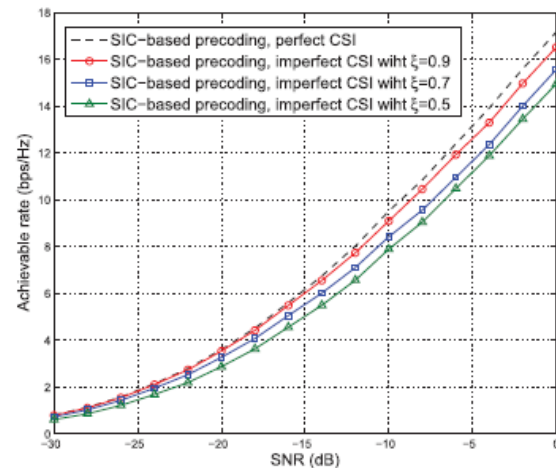


Fig. 7. Impact of imperfect CSI on SIC-based hybrid precoding for an $NM \times K = 64 \times 16$ ($N = 8$) mmWave MIMO system.

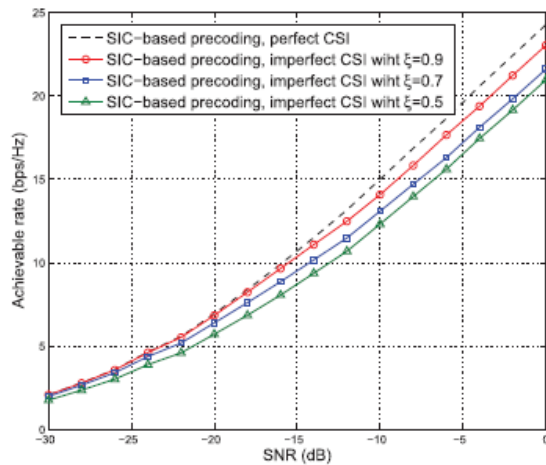


Fig. 8. Impact of imperfect CSI on SIC-based hybrid precoding for an $NM \times K = 128 \times 32$ ($N = 16$) mmWave MIMO system.

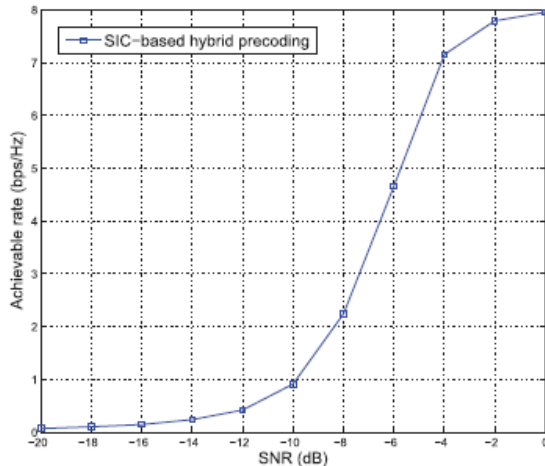


Fig. 9. Achievable rate of SIC-based hybrid precoding with finite-alphabet inputs, where $N = 8$, $NM = K = 64$, and BSPK is adopted.

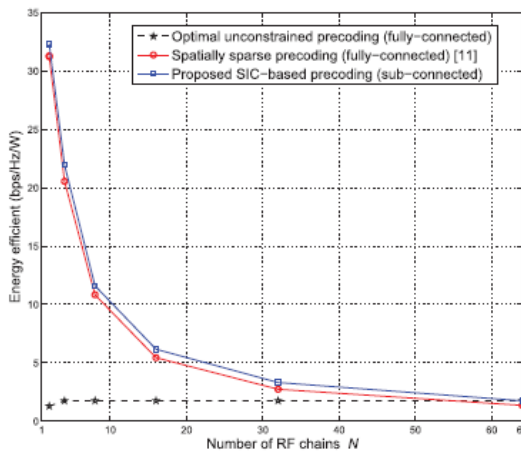


Fig. 10. Energy efficiency comparison against the numbers of RF chains N , where $NM = K = 64$.

V. CONCLUSION

In this paper, we tend to planned a SIC-based hybrid precoding with sub-connected design for MM Wave MIMO systems. We tend to initial showed that the overall doable rate improvement downside with non-convex constraints are often rotten into a series of sub-rate improvement issues, every of that solely considers one sub-antenna array. Then, we tend to prove that the sub-rate improvement downside of every sub-antenna array are often resolved by merely seeking a precoding vector sufficiently near the at liberty best resolution. Finally, a low-complexity rule was planned to appreciate SIC-based precoding while not the sophisticated SVD and matrix operation. Quality analysis showed that the quality of the planned SIC-based hybrid precoding is just concerning 100% of that of the recently planned spatially distributed precoding with fully-connected design in typical mmWave MIMO system. Simulation results verified the near-optimal performance and high energy potency of the planned SIC-based hybrid precoding. Our additional work can specialise in the restricted feedback state of affairs, wherever the angles of PSs area unit quantified.

VI. REFERENCES

- [1] T. Bai, A. Alkhateeb, and R. Heath, "Coverage and capacity of millimeter-wave cellular networks," *IEEE Commun. Mag.*, vol. 52, no. 9, pp. 70–77, Sep. 2014.
- [2] T. L. Marzetta, "Noncooperative cellular wireless with unlimited numbers of base station antennas," *IEEE Trans. Wireless Commun.*, vol. 9, no. 11, pp. 3590–3600, Nov. 2010.
- [3] Z. Pi and F. Khan, "An introduction to millimeter-wave mobile broadband systems," *IEEE Commun. Mag.*, vol. 49, no. 6, pp. 101–107, Jun. 2011.
- [4] F. Ruseket et al., "Scaling up MIMO: Opportunities and challenges with very large arrays," *IEEE Signal Process. Mag.*, vol. 30, no. 1, pp. 40–60, Jan. 2013.
- [5] L. Wei, R. Q. Hu, Y. Qian, and G. Wu, "Key elements to enable millimeterwave communications for 5G wireless systems," *IEEE Wireless Commun.*, vol. 21, no. 6, pp. 136–143, Dec. 2014.
- [6] M. Samimiet al., "28 GHz angle of arrival and angle of departure analysis for outdoor cellular communications using steerable beam antennas in New York City," in *Proc. IEEE Veh. Technol. Conf. (VTC Spring'13)*, May 2013, pp. 1–6.
- [7] A. Alkhateeb, J. Mo, N. González-Prelcic, and R. Heath, "MIMO precoding and combining solutions for millimeter-wave systems," *IEEE Commun. Mag.*, vol. 52, no. 12, pp. 122–131, Dec. 2014.
- [8] B. Yin et al., "High-throughput beamforming receiver for millimeterwave mobile communication," in *Proc. IEEE*

- Global Commun. Conf.(GLOBECOM'13), Dec. 2013, pp. 3697–3702.
- [9] P. Amadori and C. Masouros, “Low RF-complexity millimeter-wave beamspace-MIMO systems by beam selection,” *IEEE Trans. Commun.*, vol. 63, no. 6, pp. 2212–2222, Jun. 2015.
- [10] S. Han, C.-L.I, Z. Xu, and C. Rowell, “Large-scale antenna systems with hybrid precoding analog and digital beamforming for millimeter wave 5G,” *IEEE Commun. Mag.*, vol. 53, no. 1, pp. 186–194, Jan. 2015.
- [11] O. El Ayach, S. Rajagopal, S. Abu-Surra, Z. Pi, and R. Heath, “Spatially sparse precoding in millimeter wave MIMO systems,” *IEEE Trans. Wireless Commun.*, vol. 13, no. 3, pp. 1499–1513, Mar. 2014.
- [12] Y. Lee, C.-H. Wang, and Y.-H. Huang, “A hybrid RF/baseband precoding processor based on parallel-index-selection matrix-inversion-bypass simultaneous orthogonal matching pursuit for millimeter wave MIMO systems,” *IEEE Trans. Signal Process.*, vol. 63, no. 2, pp. 305–317, Jan. 2015.
- [13] C.-E. Chen, “An iterative hybrid transceiver design algorithm for millimeter wave MIMO systems,” *IEEE Wireless Commun. Lett.*, vol. 4, no. 3, pp. 285–288, Jun. 2015.
- [14] J. A. Tropp and A. C. Gilbert, “Signal recovery from random measurements via orthogonal matching pursuit,” *IEEE Trans. Inf. Theory*, vol. 53, no. 12, pp. 4655–4666, Dec. 2007.
- [15] W. Roh et al., “Millimeter-wave beamforming as an enabling technology for 5G cellular communications: Theoretical feasibility and prototype results,” *IEEE Commun. Mag.*, vol. 52, no. 2, pp. 106–113, Feb. 2014.
- [16] T. Kim, J. Park, J.-Y. Seol, S. Jeong, J. Cho, and W. Roh, “Tens of Gbps support with mmWave beamforming systems for next generation communications,” in *Proc. IEEE Global Commun. Conf. (GLOBECOM'13)*, Dec. 2013, pp. 3685–3690.
- [17] C. Kim, J. S. Son, T. Kim, and J.-Y. Seol, “On the hybrid beamforming with shared array antenna for mmWave MIMO-OFDM systems,” in *Proc. IEEE WCNC'14*, Apr. 2014.
- [18] C. A. Balanis, *Antenna Theory: Analysis and Design*. Hoboken, NJ, USA: Wiley, 2012.
- [19] D. Schneider, “Could supercomputing turn to signal processors (again)?” *IEEE Spectr.*, vol. 49, no. 10, pp. 13–14, Oct. 2012.
- [20] S. Han, C.-L.I, Z. Xu, and S. Wang, “Reference signals design for hybrid analog and digital beamforming,” *IEEE Commun. Lett.*, vol. 18, no. 7, pp. 1191–1193, Jul. 2014.
- [21] Y.-C. Liang, E. Y. Cheu, L. Bai, and G. Pan, “On the relationship between MMSE-SIC and BI-GDFE receivers for large multiple-input multiple-output channels,” *IEEE Trans. Signal Process.*, vol. 56, no. 8, pp. 3627–3637, Aug. 2008.
- [22] S. Hur, T. Kim, D. Love, J. Krogmeier, T. Thomas, and A. Ghosh, “Millimeter wave beamforming for wireless backhaul and access in small cell networks,” *IEEE Trans. Commun.*, vol. 61, no. 10, pp. 4391–4403, Oct. 2013.
- [23] C. Xiao, Y. R. Zheng, and Z. Ding, “Globally optimal linear precoders for finite alphabet signals over complex vector Gaussian channels,” *IEEE Trans. Signal Process.*, vol. 59, no. 7, pp. 3301–3314, Apr. 2011.
- [24] Y. Wu, C. Xiao, X. Gao, J. D. Matyjas, and Z. Ding, “Linear precoder design for MIMO interference channels with finite-alphabet signaling,” *IEEE Trans. Commun.*, vol. 61, no. 9, pp. 3766–3780, Sep. 2013.
- [25] F. Zhu, F. Gao, M. Yao, and H. Zou, “Joint information- and jamming beamforming for physical layer security with full duplex base station,” *IEEE Trans. Signal Process.*, vol. 62, no. 24, pp. 6391–6401, Dec. 2014.
- [26] A. Alkhateeb, O. El Ayach, G. Leus, and R. W. Heath, “Hybrid precoding for millimeter wave cellular systems with partial channel knowledge,” in *Proc. IEEE Inf. Theory Appl. Workshop (ITA'13)*, 2013, pp. 1–5.
- [27] M. Tao and R. Wang, “Linear precoding for multi-pair two-way MIMO relay systems with max-min fairness,” *IEEE Trans. Signal Process.*, vol. 60, no. 10, pp. 5361–5370, Oct. 2012.
- [28] G. H. Golub and C. F. Van Loan, *Matrix Computations*. Baltimore, USA: JHU Press, 2012.
- [29] Å. Björck, “Numerical methods in matrix computations,” Berlin, German: Springer, 2015.
- [30] O. El Ayach, R. W. Heath, S. Rajagopal, and Z. Pi, “Multimode precoding in millimeter wave MIMO transmitters with multiple antenna sub-arrays,” in *Proc. IEEE Global Commun. Conf. (GLOBECOM'13)*, Dec. 2013, pp. 3476–3480.
- [31] A. Alkhateeb, O. El Ayach, G. Leus, and R. Heath, “Channel estimation and hybrid precoding for millimeter wave cellular systems,” *IEEE J. Sel. Topics Signal Process.*, vol. 8, no. 5, pp. 831–846, Oct. 2014.
- [32] Y. Wu, C. Xiao, Z. Ding, X. Gao, and S. Jin, “Linear precoding for finite alphabet signaling over MIMO wiretap channels,” *IEEE Trans. Veh. Technol.*, vol. 61, no. 6, pp. 2599–2612, Jul. 2012.
- [33] S. Cui, A. J. Goldsmith, and A. Bahai, “Energy-constrained modulation optimization,” *IEEE Trans. Wireless Commun.*, vol. 4, no. 5, pp. 2349–2360, Sep. 2005.
- [34] C. Masouros, M. Sellathurai, and T. Rantarahaj, “Computationally efficient vector perturbation using thresholded optimization,” *IEEE Trans. Commun.*, vol. 61, no. 5, pp. 1880–1890, May 2013.
- [35] T. S. Rappaport, J. N. Murdock, and F. Gutierrez, “State of the art in 60-GHz integrated circuits and systems for wireless communications,” *Proc. IEEE*, vol. 99, no. 8, pp. 1390–1436, Aug. 2011.
- [36] D. Tse and P. Viswanath, *Fundamentals of Wireless Communication*. Cambridge, U.K.: Cambridge Univ. Press, 2005.